

## O<sub>2</sub> sensing is preserved in mice lacking the gp91 phox subunit of NADPH oxidase

(K<sub>v</sub> channels/iberiotoxin/hypoxic pulmonary vasoconstriction/O<sub>2</sub> radicals/chronic granulomatous disease)

STEPHEN L. ARCHER\*<sup>†</sup>, HELEN L. REEVE<sup>†‡</sup>, EVANGELOS MICHELAKIS\*, LAKSHMI PUTTAGUNTA<sup>§</sup>, ROSS WAITE\*, DANIEL P. NELSON<sup>†</sup>, MARY C. DINAUER<sup>¶</sup>, AND E. KENNETH WEIR<sup>†||</sup>

\*Department of Medicine, Division of Cardiology, and <sup>§</sup>Department of Pathology, University of Alberta, Edmonton, Canada T69 2B7; <sup>†</sup>Department of Medicine, Veterans Administration Medical Center, Minneapolis, MN 55417; <sup>‡</sup>Department of Physiology, University of Minnesota, Minneapolis, MN 55455; and <sup>¶</sup>Department of Pediatrics, Indiana University School of Medicine, Indianapolis, IN 46202

Communicated by Paul B. Beeson, University of Washington, Redmond, WA, April 19, 1999 (received for review January 15, 1999)

**ABSTRACT** The rapid response to hypoxia in the pulmonary artery (PA), carotid body, and ductus arteriosus is partially mediated by O<sub>2</sub>-responsive K<sup>+</sup> channels. K<sup>+</sup> channels in PA smooth muscle cells (SMCs) are inhibited by hypoxia, causing membrane depolarization, increased cytosolic calcium, and hypoxic pulmonary vasoconstriction. We hypothesize that the K<sup>+</sup> channels are not themselves “O<sub>2</sub> sensors” but rather respond to the reduced redox state created by hypoxic inhibition of candidate O<sub>2</sub> sensors (NADPH oxidase or the mitochondrial electron transport chain). Both pathways shuttle electrons from donors, down a redox gradient, to O<sub>2</sub>. Hypoxia inhibits these pathways, decreasing radical production and causing cytosolic accumulation of unused, reduced, freely diffusible electron donors. PASM C K<sup>+</sup> channels are redox responsive, opening when oxidized and closing when reduced. Inhibitors of NADPH oxidase (diphenyleneiodonium) and mitochondrial complex 1 (rotenone) both inhibit PASM C whole-cell K<sup>+</sup> current but lack the specificity to identify the O<sub>2</sub>-sensor pathway. We used mice lacking the gp91 subunit of NADPH oxidase [chronic granulomatous disease (CGD) mice] to assess the hypothesis that NADPH oxidase is a PA O<sub>2</sub>-sensor. In wild-type lungs, gp91 phox and p22 phox subunits are present (relative expression: macrophages > airways and veins > PASM Cs). Deletion of gp91 phox did not alter p22 phox expression but severely inhibited activated O<sub>2</sub> species production. Nonetheless, hypoxia caused identical inhibition of whole-cell K<sup>+</sup> current (in PASM Cs) and hypoxic pulmonary vasoconstriction (in isolated lungs) from CGD vs. wild-type mice. Rotenone vasoconstriction was preserved in CGD mice, consistent with a role for the mitochondrial electron transport chain in O<sub>2</sub> sensing. NADPH oxidase, though a major source of lung radical production, is not the pulmonary vascular O<sub>2</sub> sensor in mice.

The pulmonary circulation is a low-resistance vascular bed. Within seconds of onset of alveolar hypoxia (1, 2), the small, muscular pulmonary arteries (PAs) serving the hypoxic area constrict. This hypoxic pulmonary vasoconstriction (HPV) diverts blood flow to better-ventilated alveoli, thereby matching ventilation to perfusion and optimizing systemic PO<sub>2</sub>. Though modified by many humoral factors, HPV is intrinsic to PA smooth muscle cells (SMCs) (3) and is most robust in small, muscular resistance arteries (4, 5). HPV is initiated by inhibition of one or more voltage-gated potassium (K<sub>v</sub>) channels in PASM Cs (5–9). This inhibition causes membrane depolarization and activation of L-type Ca<sup>2+</sup> channels and raises cytosolic Ca<sup>2+</sup> levels, [Ca<sup>2+</sup>]<sub>i</sub>, thereby causing vasoconstriction (2). This mechanism is similar to that described in the hypoxic

response of carotid body type 1 cell (10), the neuroepithelial body (11), and pheochromocytoma (PC 12) cells (12). Although significant progress has been made in identifying the K<sub>v</sub> channels that respond to hypoxia (K<sub>v1.5</sub>/K<sub>v2.1</sub>) (8, 9) and K<sub>v1.2</sub> (13), the molecular origins of the redox signal that serves as a “sensor” is unknown.

There is substantial evidence that K<sup>+</sup> channel activity and vascular tone can be modulated by reducing and oxidizing agents. The importance of reduction-oxidation (redox) potential of key sulfhydryl groups in the gating mechanisms of certain K<sub>v</sub> channels appears related to the presence of cysteine groups in the channel (14). In PASM Cs, oxidants [such as *t*-butyl hydroperoxide, reduced/oxidized glutathione (GSH) (GSSG), and diamide; ref. 2] increase opening of K<sub>v</sub> channels causing membrane hyperpolarization and relaxation. Conversely, reduction (caused by GSH and electron shuttling agents, such as duroquinone) causes channel inhibition, membrane depolarization, and vasoconstriction (2, 15).

Several possible sensors have been proposed, each of which depends on modulation of cell redox state in PASM Cs in proportion to PO<sub>2</sub>, usually a more reduced state in hypoxia and more oxidized state in normoxia: (i) production of activated O<sub>2</sub> species (AOS), radicals, and H<sub>2</sub>O<sub>2</sub> by membrane-bound NADPH oxidase; and (ii) accumulation of freely diffusible redox couples (e.g., GSH/GSSG and NADH/NAD<sup>+</sup>) because of changes in the function of the mitochondrial electron transport chain (ETC).

Some evidence indicates that NAD(P)H oxidase could be the O<sub>2</sub> sensor in the pulmonary vasculature (16–18), carotid body (19), and neuroepithelial body. Marshall *et al.* (20) found a functional NADPH oxidase, containing the gp91 phox component, in small rat PAs. However, in their study, hypoxia paradoxically increased radical production measured in cultured cells. In contrast, most reports in which radical formation is measured in intact PAs or isolated lungs find that AOS production decreases as PO<sub>2</sub> falls within the physiological range (21–23). Others have found an NAD(P)H oxidase in conduit PASM Cs and also have shown that hypoxia acutely inhibits radical production (17, 18). The abbreviations NADPH and NAD(P)H refer to the enzyme's preferred substrate. NADPH oxidase preferentially uses NADPH as an electron donor; NAD(P)H indicates a form of the enzyme that

Abbreviations: PA, pulmonary artery; SMC, smooth muscle cell; CGD, chronic granulomatous disease; ETC, electron transport chain; HPV, hypoxic pulmonary vasoconstriction; K<sub>v</sub>, voltage-gated potassium channel; I<sub>K</sub>, whole-cell K<sup>+</sup> current; E<sub>M</sub>, membrane potential; GSH/GSSG reduced/oxidized glutathione; IBTX, iberiotoxin; AOS, activated O<sub>2</sub> species; PMA, phorbol myristate acetate; DPI, diphenyleneiodonium; PVR, pulmonary vascular resistance; PAP, pulmonary artery pressure; Ang II, angiotensin II; 4-AP, 4-aminopyridine.

<sup>||</sup>To whom reprint requests should be addressed at: Veterans Administration Medical Center (111C), One Veterans Drive, Minneapolis, MN 55417. e-mail: weirx002@maroon.tc.umn.edu.

The publication costs of this article were defrayed in part by page charge payment. This article must therefore be hereby marked “advertisement” in accordance with 18 U.S.C. §1734 solely to indicate this fact.

PNAS is available online at www.pnas.org.

preferentially accepts electrons from NADH, but which may use NADPH, at higher concentrations.

An alternative theory, the redox hypothesis (2, 24, 25), suggests that the mitochondrial ETC, through its effects on cytosolic redox state, is the O<sub>2</sub> sensor (25, 26). Inhibitors of the proximal mitochondrial ETC, e.g., rotenone, functionally obstruct electron transport, leading to proximal (cytosolic) accumulation of electron donors, thereby shifting the redox state to a reduced position. Rotenone mimics hypoxia in that it reduces whole-cell K<sup>+</sup> current (*I<sub>K</sub>*) (25, 27), causes pulmonary vasoconstriction (25, 28), and activates the carotid body (26). It remains unclear whether it is the AOS themselves or a parallel change in the cytosolic redox state that serves as a sensor. Therefore, we turned to a genetic model to examine the role of NADPH oxidase as an O<sub>2</sub> sensor in the PA.

NADPH oxidase is present in phagocytes, carotid body type 1 cells (19), neuroepithelial bodies (29), PASMCs (18, 20), and endothelial cells (30). It includes a membrane-bound flavocytochrome containing two subunits, gp91 phox and p22 phox, and the cytosolic proteins p47 phox and p67 phox, which bind to the flavocytochrome to form the active enzyme complex (31–33). Much of the evidence indicating NADPH oxidase may be an O<sub>2</sub> sensor rests on the use of diphenyleneiodonium (DPI), a nonspecific inhibitor of flavoprotein-containing enzymes, including membrane oxidases (NADH and NADPH) (34), nitric oxide synthase (35), and complex 1 of the mitochondrial ETC (36). Although DPI inhibits *I<sub>K</sub>*, it reduces HPV (16), possibly because it blocks L-type Ca<sup>2+</sup> channels (37). For all of these reasons, DPI is a poor tool for establishing the physiological role of NADPH oxidase in regulating vascular tone.

## METHODS

**Isolated Mouse Lung Model.** To study the effects of hypoxia on pulmonary vascular resistance (PVR) [mean pulmonary artery pressure (PAP)-left atrial pressure ÷ flow], an isolated mouse lung model was developed. In this model, flow is held constant (3 ml/min), left atrial pressure is kept near 0 mmHg, and mean PA pressure is measured. Because flow is constant, PAP directly reflects PVR. Chronic granulomatous disease (CGD) and wild-type (C57BL/6J) mice were obtained from M.C.D. and The Jackson Laboratory. Mice were anesthetized with Nembutal (50 mg/kg i.p.), and a tracheotomy was performed by using a PE90 tube (Curtin Matheson Scientific, Houston). The lung was ventilated at 163 breaths/min (Harvard Rodent Ventilator 683, South Natick, MA) with a tidal volume of 0.15 ml. A thoracotomy was performed, and the PA was cannulated by using a dual lumen perfusion catheter (PE60 perfusion catheter, internal/external diameter, 0.030/0.048 in; PE10 pressure catheter, internal/external diameter, 0.011/0.024 in). The left atrium was cannulated by using a PE190 cannula (internal/external diameter, 0.047/0.067 in). The lungs were suspended in a humidified chamber and perfused (LKB Pump 2115). Lungs were ventilated with normoxic (20% O<sub>2</sub>) or hypoxic (2.5% O<sub>2</sub>) gas (5% CO<sub>2</sub>, balance N<sub>2</sub> for each). The perfusate [20 ml of Krebs solution (22.6 mM NaHCO<sub>3</sub>, 119 mM NaCl, 50 mM sucrose, 4.7 mM KCl, 1.17 mM MgSO<sub>4</sub>, 1.18 mM KH<sub>2</sub>PO<sub>4</sub>, 5.5 mM D-glucose, 3.2 mM CaCl<sub>2</sub>) with 4% albumin at 38°C] contained the cyclooxygenase inhibitor, meclofenamate (5 μM), which enhances HPV by inhibiting production of vasodilator prostanooids (38).

**Lung Protocol A.** The goal of this protocol was to compare AOS production and PVR (measured simultaneously in the isolated lung) in wild and CGD groups (meclofenamate in perfusate; wild = 9, CGD = 9). Pressure-flow relationships were studied over the range of 1 to 11 ml/min. After 10 min of equilibration, angiotensin II (AII) was given (0.15 μg, PA bolus). AII was given because it “primes” the PAs, increasing

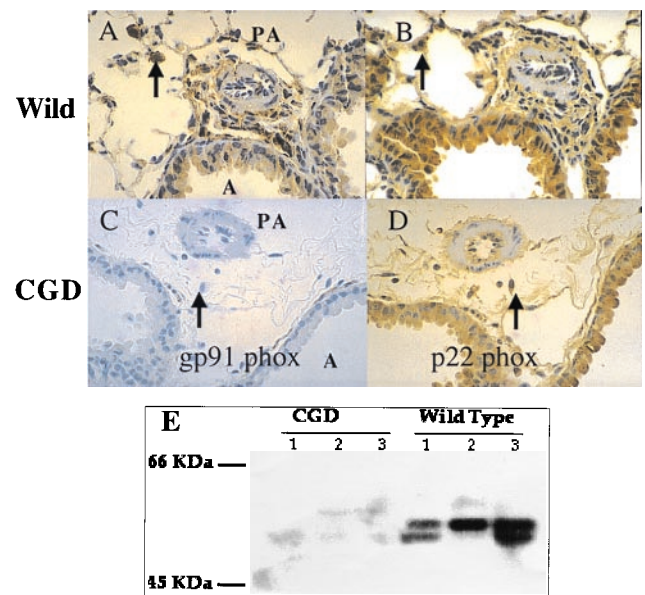


FIG. 1. gp91 phox and p22 phox are present in the lung. gp91 phox (A) and p22 phox (B) are present in wild-type mice (immunohistochemistry in brown, counterstain blue). Controls lacking primary antibody are completely negative (not shown). As expected, the gp91 phox (C), but not the p22 phox (D), is absent in the CGD mouse. Lack of gp91 phox in C reveals the hematoxylin counterstain. Qualitative grading of the intensity of expression of gp91 phox by blinded observers was: alveolar macrophages (arrows), 4+; alveolar epithelium airways, 3+; pulmonary veins, 3+; large PAs, 2+; and small PAs, 1+. (E) Immunoblots show a typical band for gp91 phox at ≈60 kDa. The gp91 phox refers to the molecular weight in human tissue, where the subunit is more heavily glycosylated.

the magnitude of HPV at doses of AII that cause only a small constriction. Also, AII-induced constriction of some arteries has been postulated to result from activation of NADPH oxidase (39). Eight minutes later, the lung was ventilated with hypoxic gas for 6 min. These cycles were repeated 4–6 times. Finally, rotenone (50 μM) was given in the PA line.

**Chemiluminescence.** In protocol A, chemiluminescence was measured “on-line” from the lung surface before (unenhanced) and after addition of luminol (50 μM) or lucigenin (50 μM) (enhanced) (22, 23). Luminol yielded similar results as lucigenin but is less specific for superoxide detection and thus we report only results with lucigenin. Lucigenin predominantly measures superoxide anion (22, 23, 40, 41), whether produced by NADPH oxidase or mitochondria (41). Lucigenin enters cells and accumulates in mitochondria (41). At the end of the protocol, 0.1–10 μM phorbol myristate acetate (PMA), an agent that stimulates radical production by NADPH oxidase, was given to assess the ability of the lung to generate a burst of AOS.

**Lung Protocol B.** The goal of this protocol was to determine whether potential differences in nitric oxide levels in CGD vs. wild-type mice might be masking intrinsic hemodynamic differences [meclofenamate + L-nitro arginine methylester (16 μM) in perfusate; wild = 5, CGD = 5]. This possibility was suggested by the fact that NO is rapidly destroyed by superoxide radicals, which CGD mice lack. Protocol B was similar to protocol A, except the response to a different “redox-dependent” vasoconstrictor, duroquinone, was tested. Duroquinone (1 μM) previously has been shown to alter electron shuttling, inhibit *I<sub>K</sub>*, and elevate PVR (15).

**Histology.** After completion of protocol A, the heart was removed and the left ventricle + septal weight was compared with the right ventricular weight. The lung was fixed in paraformaldehyde, and histology was assessed (42).

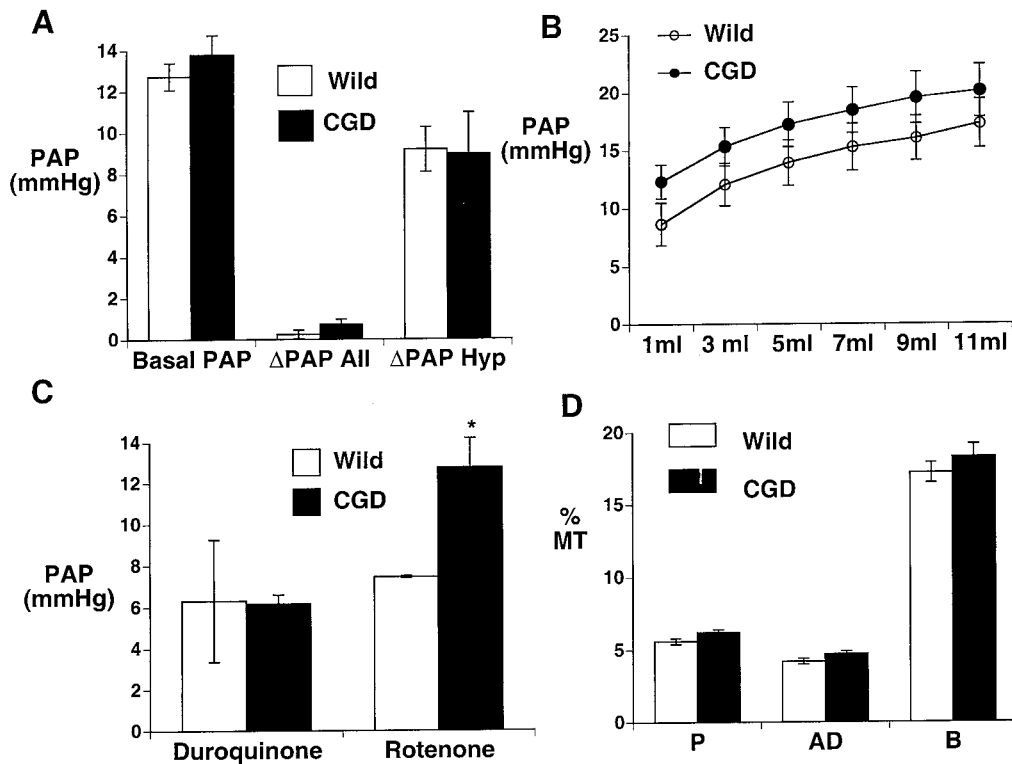


FIG. 2. HPV is preserved and there is no pulmonary hypertension in CGD mice. (A) There are no intergroup differences in HPV or the constrictor response to AII in isolated mouse lungs (perfusate contains L-nitro arginine methylester and meclofenamate). (B) There are no intergroup differences in the pressure/flow relationship in isolated mouse lungs (perfusate contains meclofenamate). (C) There are no intergroup differences in duroquinone-induced constriction in isolated mouse lungs (perfusate contains meclofenamate and L-nitro arginine methylester). In separate experiments, rotenone vasoconstriction is enhanced in isolated lungs from CGD vs. wild-type mice ( $P < 0.05$ ), (perfusate contains meclofenamate). (D) There is no medial hypertrophy of PAs on light microscopy. P, AD, and B refer to the size of PA studied as related to the associated airway (parenchymal, alveolar duct, and bronchial, respectively).

**Immunohistochemistry and Immunoblotting.** Proteins ( $n = 3$  lungs/group,  $75 \mu\text{g}$  per lane) were separated on 7.5% (p22 phox) or 15% (gp91 phox) SDS/PAGE gels and subsequently electroblotted onto nitrocellulose. The filters then were blocked with Tris-buffered saline containing Tween20 and Blotto (50 mM Tris-HCl, pH 7.4/100 mM NaCl/5% nonfat dry milk) for 1 hr at  $25^\circ\text{C}$ . Primary antibodies (1:1,000 dilution) were incubated with the blots for 4 hr at  $25^\circ\text{C}$ . After washing, secondary antibodies (1:3,000, goat anti-mouse or anti-rabbit, horseradish peroxidase linked; Pierce) were diluted in Blotto and applied for 1.5 hr at  $25^\circ\text{C}$ . The immunoblots were developed by using ECL reagents (Amersham Pharmacia) and exposed to BioMax-MR film (Kodak).

Immunohistochemistry was performed on paraffin-embedded, formaldehyde-fixed lungs ( $n = 3$  lungs/group) counterstained with hematoxylin. Tissue was exposed to primary antibody (1/150 dilution) for 16 hr at  $4^\circ\text{C}$  and biotinylated secondary antibody for 20 min at  $25^\circ\text{C}$  (1/20 dilution of Link Biogenex Laboratories, San Ramon, CA). After exposure to streptavidin peroxidase (Label 20 min,  $37^\circ\text{C}$ ), they were revealed with diaminobenzidine (Biogenex Laboratories).

**Cell Isolation.** CGD or wild mice were anesthetized, PAs (third-fourth division) were dissected, and SMCs were dissociated as described (5) for amphotericin-perforated, whole-cell, patch-clamp studies (5).

**Electrophysiology.** Cells were perfused (2 ml/min) with a normoxic solution of composition 115 mM NaCl, 25 mM  $\text{NaHCO}_3$ , 4.2 mM KCl, 1.2 mM  $\text{KH}_2\text{PO}_4$ , 1.5 mM  $\text{CaCl}_2$ , 10 mM Hepes 10 (pH 7.4,  $\text{PO}_2 = 120$  mmHg created by bubbling with 20%  $\text{O}_2$ /3.5%  $\text{CO}_2$ /balance  $\text{N}_2$ ). Electrodes (resistance 1–5 M $\Omega$ ) were filled with a solution containing 140 mM KCl, 1.0 mM  $\text{MgCl}_2$ , 10 mM Hepes, 5 mM EGTA, and 120  $\mu\text{g}/\text{ml}$  amphotericin B, pH 7.2. Capacitance was corrected, and

perforation was monitored by changes in membrane potential ( $E_M$ ) and series resistance. Hypoxic solutions ( $\text{PO}_2 = 40$  mmHg) were bubbled with 3.5%  $\text{CO}_2$ , balance  $\text{N}_2$ . Current density was calculated by dividing average, whole-cell  $I_K$  by cell capacitance (pA/pF). Cells were voltage-clamped at a holding potential of  $-70$  mV, and currents were evoked by voltage steps up to  $+50$  mV by using test pulses of 200-ms duration at 0.1 Hz. Currents were filtered at 1 kHz and sampled at 2 or 4 kHz. To record  $E_M$ , cells were held at their resting potential in current-clamp mode. All data were recorded at  $32^\circ\text{C}$ , unless otherwise stated, and analyzed by using PCLAMP 6.03 software (Axon Instruments, Foster City, CA). The effect of 4-aminopyridine (4-AP, 1 mM), a preferential  $\text{K}_v$  inhibitor, and tetraethylammonium (5 mM), a preferential inhibitor of calcium-sensitive  $\text{K}^+$  channels ( $\text{K}_{Ca}$ ), was assessed in wild and CGD PASMCS ( $n = 5$  each). In additional experiments (seven CGD, four wild), the effect of hypoxia on  $I_K$  was assessed in SMCs from resistance PAs at  $25^\circ\text{C}$ , after specifically inhibiting large-conductance  $\text{K}_{Ca}$  channels with 100 nM iberiotoxin (IBTX).

**Endothelium-Denuded Rat PA Rings.** These experiments evaluated AOS production by the arterial media. Fourth-division PA rings from adult, male Sprague-Dawley rats ( $n = 8$ ) were studied in Krebs solution containing 10 mM Hepes at  $39^\circ\text{C}$ . Lucigenin-enhanced ( $5 \times 10^{-5}$  M) chemiluminescence was measured by using a liquid scintillation analyzer (Packard 1900CA). Mean normoxic and hypoxic  $\text{PO}_2$ s were 133 mmHg and 36 mmHg, respectively. To determine the source of AOS production, DPI (1  $\mu\text{M}$ ) was added to an additional group of normoxic and hypoxic rings ( $n = 8$  each).

**Drugs and Statistics.** Values are expressed as the mean  $\pm$  SEM. Comparison between two and three groups used Student's  $t$  test and a factorial ANOVA, respectively. Repeated

measures ANOVA was used for assessment of pressure-flow relationships. Fisher's probable least significant differences test was performed for post hoc comparisons. All drugs were from Sigma except IBTX (Peptides International) and DPI (Research Biochemicals, Natick, MA). All drugs were dissolved in saline (except rotenone, DPI, and PMA, which were dissolved in DMSO). Appropriate vehicle controls were performed.

## RESULTS

**General.** The CGD mice were smaller than the wild type ( $22 \pm 1$  g vs.  $28 \pm 2$ ,  $P = .005$ ). Histology showed no evidence of pneumonia or medial hypertrophy. The left ventricle + septal weight compared to right ventricular weight was  $4.6 \pm 0.3$  vs.  $4.0 \pm 0.3$  in wild and CGD mice, indicating absence of right ventricular hypertrophy.

**Immunohistochemistry.** Both gp91 phox and p22 phox were abundant in wild-type lungs (Fig. 1). As expected, the gp91 phox, but not the p22 phox, was absent in the CGD mouse. The expression of p22 phox was unaltered by the mutation of gp91 phox. Immunohistochemistry shows that both p22 phox and gp91 phox are most abundant in the alveolar macrophages (4+) and airway epithelium (3+) (Fig. 1). Both subunits were found in greater quantities in the large pulmonary veins (3+, not shown) than in similar-sized PAs (2+). In the media of the small PAs that contribute most to HPV, there was 1+ gp91 phox and no p22 phox; however, p22phox was evident in the endothelium of these resistance arteries (1–2+, Fig. 1).

**Isolated Mouse Lung.** There were no intergroup differences in normoxic perfusion pressure, pressure-flow relationships, HPV, or AII constriction (Fig. 2). NOS inhibition enhanced HPV ( $P < 0.01$ ) equally in both groups (data not shown). Duroquinone caused similar vasoconstriction in CGD and wild-type mice (Fig. 2). Rotenone caused greater vasoconstriction in CGD than in wild-type mice ( $P < 0.05$ , Fig. 2).

**AOS.** CGD mice made less AOS than wild-type mice, whether measured in the unenhanced state, in the presence of lucigenin, or after stimulation with PMA (Fig. 3). The vasoconstrictor response to PMA was similar in both groups, despite the differences in radical production (not shown). AOS production was detectable in rat resistance PA rings in the absence of endothelium (Fig. 3). Both hypoxia and DPI inhibited normoxic AOS production. However, hypoxia diminished AOS even after DPI, suggesting there is an  $O_2$ -sensitive, DPI-insensitive source of AOS in rat resistance PAs.

**Electrophysiology.** Current density,  $I_K$  and  $E_M$ , were nearly identical in PSMCs from CGD and wild-type mice (Fig. 4A and B). In CGD PSMCs,  $I_K$  was partially inhibited by low doses of the  $K_v$  channel blocker, 4-AP, at negative  $E_M$  (Fig. 4C). In contrast, tetraethylammonium only inhibited  $I_K$  at test potentials positive to +20 mV, consistent with the positive activation threshold of  $K_{Ca}$  channels (Fig. 4D). Acute hypoxia rapidly inhibited  $I_K$  in both wild-type and CGD mice, even in the presence of IBTX (Fig. 4E and F).

## DISCUSSION

There is good reason to hypothesize that a NADPH oxidase containing gp91 phox could be an  $O_2$  sensor. It appears that most  $O_2$ -responsive cell types contain a similar form of the oxidase, containing the gp91 phox component. For example, the carotid body type 1 cell and neuroepithelial body have an NADPH oxidase similar or identical to that of neutrophils (containing both p22 phox and gp91 phox) (43). However, CGD mice, with a confirmed absence of gp91 phox, have preserved  $O_2$  sensing, manifest by robust HPV and hypoxia-inhibited  $I_K$  (Figs. 1–3). The knockout of gp91 phox rendered the NADPH oxidase complex nonfunctional, despite the persistence of normal p22 phox expression (Figs. 1 and 3). Despite

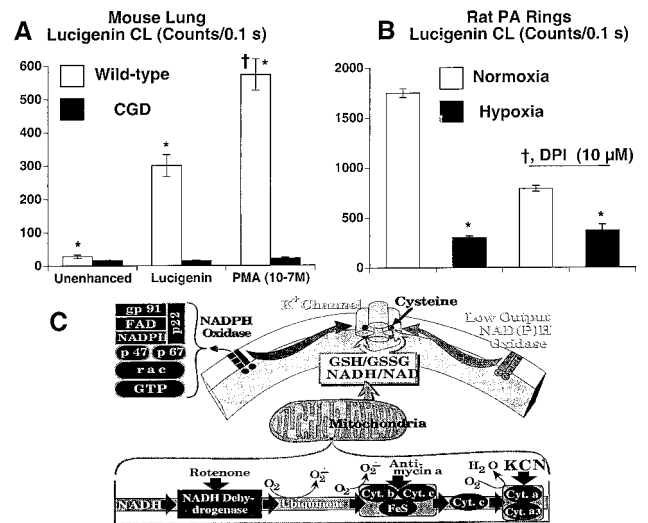


Fig. 3. NADPH oxidase is functionally disrupted in the lungs of CGD mice. (A) Isolated lungs from CGD mice produce less AOS than wild-type mice, whether measured unenhanced or with lucigenin (\*,  $P < 0.05$ ). PMA increases lucigenin chemiluminescence in lungs from wild-type, but not CGD, mice (†,  $P < 0.05$ ). (B) Lucigenin-enhanced chemiluminescence is diminished by acute hypoxia and by DPI in rat PA rings (fourth division) denuded of endothelium. \*,  $P < 0.05$  value differs from normoxia. (C) Schematic of two competing theories for redox regulation of  $K^+$  channels. In one, a gp91 phox containing NADPH produces AOS, which modulate channel function through effects on critical channel cysteine groups. In the other, inhibition of mitochondrial complex 1 leads to accumulation of cytosolic reducing equivalents, which in turn inhibit the  $K^+$  channel by interaction with its cysteine groups.

the virtual absence of AOS in CGD mice, the smooth muscle  $I_K$  and  $E_M$  were similar in CGD vs. wild-type mice (Fig. 4). More importantly, normoxic PAP, pressure-flow relationships, and vascular morphology were virtually identical between groups (Fig. 2). These observations refute the concept that NADPH oxidase serves as a vascular  $O_2$  sensor that regulates PVR through its effects on  $K^+$  channels. Moreover, given that HPV is intrinsic to the PASM (3), the tissue distribution of both gp91 phox and p22 phox is not consistent with a role as a vascular  $O_2$  sensor. In wild-type lungs, both subunits are most abundant in the airways and pulmonary veins, with much less expression in the PAs. Only gp91 phox is found in the SMCs of resistance PAs; whereas p22 phox is evident only in the endothelium of these arteries.

There is other evidence against a role of NADPH oxidase functioning as a "universal"  $O_2$  sensor. Wenger *et al.* (44) found NADPH-deficient cells (lacking either the p22 phox or gp91 phox) had normal expression of hypoxia-inducible genes. They examined the induction of vascular endothelial growth factor (VEGF) by hypoxia in NADPH oxidase-deficient cells and found hypoxia increased VEGF expression normally.

This study proves that a gp91 phox containing NADPH oxidase is the major source of AOS in the lung, as measured by chemiluminescence (Fig. 3). Indeed, there was little, if any, residual chemiluminescence/radical production to attribute to other sources, such as a low-output variants of the oxidase. Recently it has been suggested that a "low-output" NAD(P)H oxidase may use the p22 phox to generate superoxide radical without requiring the gp91 phox component (45, 46). Several groups have found isoforms resembling NADPH oxidase that are distinct from those in neutrophils and macrophages. These isoforms use NADH as a substrate (in preference to NADPH) (17, 18), and they make radicals at a low basal rate, unlike the "burst" pattern of radical production seen in neutrophils. This low production of radicals has earned them the classification

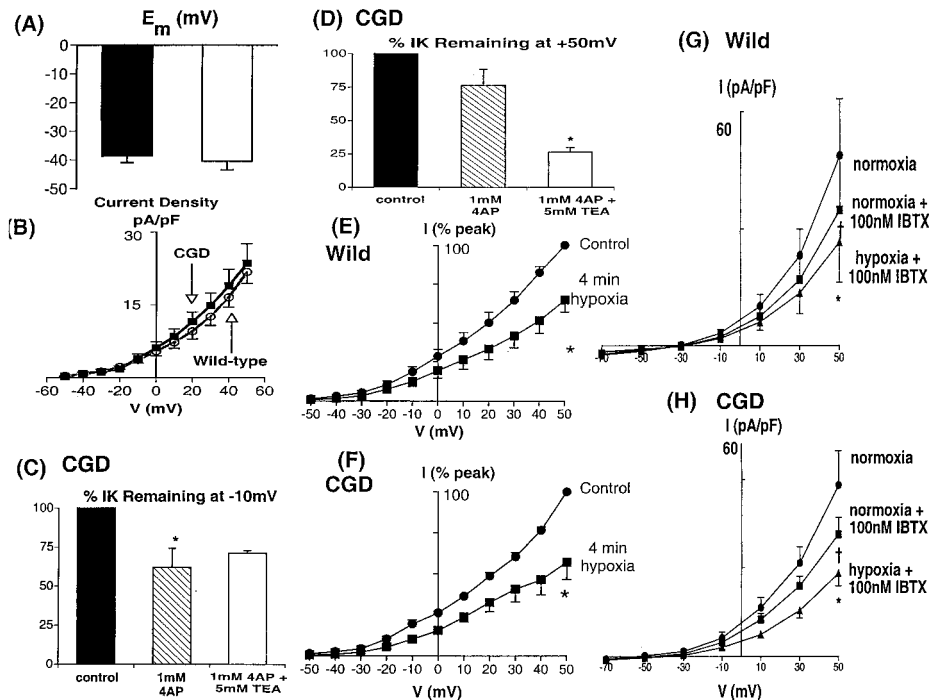


FIG. 4.  $E_m$  and  $I_K$  are similar in resistance PSMCs from wild-type and CGD mice (A) Resting  $E_m$  is similar in wild-type (filled bar) and CGD (empty bar) PSMCs. (B) Normoxic current density is similar in wild-type and CGD PSMCs. (C and D) In PSMCs from CGD mice, 4-AP, a  $K_v$  channel inhibitor, reduces  $I_K$  at negative potentials ( $-10$  mV, C, \*,  $P < 0.05$ ). Tetraethylammonium (TEA) inhibits  $I_K$  only at positive potentials, where  $K_{Ca}$  channels are active (\*,  $P < 0.05$ , D). (E and F) Four minutes of acute hypoxia inhibits  $I_K$  ( $n = 4$  cells/group, \*,  $P < 0.01$ ). (G and H) In separate experiments, 4 min of acute hypoxia inhibits  $I_K$  even after specifically inhibiting large conductance  $K_{Ca}$  channels with IBTX. This finding suggests the hypoxia-sensitive current is at least partially  $K_v$  current ( $\dagger$ , \*  $P < 0.05$  IBTX and hypoxia inhibit  $I_K$ , respectively).

of low-output isoforms. However, this concept remains controversial because it has not been conclusively proven that the gp91 phox component is absent from this isoform in vascular myocytes (46), although renal mesangial cells do have a low-output form of the oxidase that lacks the gp91 phox component (32). In support of the importance of the gp91 phox component, several cells, other than neutrophils, do express and functionally use gp91 phox, including human endothelial cells (47), type 1 carotid body cells (29), neuroepithelial cells (29), PSMCs (20), and arguably, even the renal mesangial cell (48).

In our study, p22 phox expression was unaltered despite virtual elimination of AOS production in CGD mice. This finding makes it improbable that in normal mouse lung NADPH oxidase can acutely make radicals solely via p22 phox. In addition, the timing of radical production ascribed to the p22 phox-dependent oxidase by Griendling *et al.* (39) appears too slow to explain  $O_2$  sensing in the PA. Acute hypoxia elevates PVR and suppresses AOS production within seconds, which is rapidly reversible (49). In contrast, the activation of NAD(P)H oxidase by AII, in systemic SMCs, causes a slow onset (minutes-hours) of sustained superoxide production (39).

An alternate  $O_2$  sensor in the PSMC is the redox ratio of freely diffusible electron donors that normally provide electrons for the mitochondrial ETC. The redox hypothesis, illustrated in Fig. 3C, is based on several observations. First, the oxidative function of mitochondria in the lung varies in proportion to  $PO_2$  (21, 22, 50). Despite the low  $K_M$  for  $O_2$  of the mitochondrial cytochromes, lung mitochondria make AOS in direct proportion to  $PO_2$  over the physiological range (51). Hypoxia impairs the transfer of electrons to the proximal ETC, which shifts the redox ratio of cytosolic couples, such as NADH/NAD and GSH/GSSG, toward the reduced forms. Second, inhibitors of the mitochondrial ETC mimic hypoxia's effects on the carotid body (e.g., they increase sinus nerve

activity) (50, 52) and the lung (e.g., cause pulmonary vasoconstriction) (25, 28). Third, the acute effects of hypoxia and mitochondrial inhibitors occur without impairment of energy generation. Metabolic uncouplers (e.g., dinitrophenol) stimulate dopamine secretion and enhanced nerve activity in the cat carotid body without lowering ATP levels (53). Likewise, in the lung, moderate hypoxia elicits HPV without ATP depletion (54). A fourth similarity between metabolic inhibitors and hypoxia is that rotenone and antimycin, but not cyanide, inhibit  $I_K$  in PSMCs and reduce lung AOS production (25, 27). This inhibition occurs despite the use of a patch pipette replete with ATP and is unaltered by glyburide, an inhibitor of the ATP-dependent  $K^+$  channel ( $K_{ATP}$ ) (25). We suggest the metabolic inhibitors constrict PAs not by depletion of high-energy phosphates or by impairing AOS production, but by accelerating the accumulation of reduced forms of redox couples in the cytosol. Certainly, the reduced forms of these freely diffusible redox couples (e.g., GSH) inhibit  $I_K$  when applied exogenously (2, 15, 27).

The evidence in favor of the mitochondrial ETC-cytosolic redox theory in the current experiment is circumstantial, but consistent with previous observations. First, duroquinone, a lipophilic synthetic analog of mitochondrial coenzyme Q that facilitates electron shuttling, caused pulmonary vasoconstriction in both wild and CGD mice (Fig. 2). Second, rotenone is one of the few vasoconstrictors that mimics hypoxia. However, there have been concerns that rotenone might not be a specific inhibitor of complex 1 of the mitochondria, in particular that it might inhibit NADPH oxidase. The fact that rotenone-induced pulmonary vasoconstriction is not diminished by lack of a functional NADPH oxidase is particularly meaningful in the CGD mouse, as its effects are unlikely to be the result of nonspecific inhibition of NADPH oxidase.

S.L.A. is supported by the Alberta Heritage Foundation for Medical Research, the Medical Research Council of Canada, the Alberta Heart

and Stroke Foundation, and the American Heart Association. E.M. is supported by the Alberta Heritage Foundation for Medical Research. E.K.W. is supported by the Department of Veterans Affairs. H.L.R. is supported by National Institutes of Health Grant R29 29182, the American Heart Association Grant, and a Giles Filley Award. M.C.D. is supported by National Institutes of Health Grant RO1 HL52565.

1. Jensen, K., Mico, A., Czartolomna, J., Latham, L. & Voelkel, N. (1992) *J. Appl. Physiol.* **72**, 2018–2023.
2. Weir, E. K. & Archer, S. L. (1995) *FASEB J.* **9**, 183–189.
3. Madden, J. A., Vadula, M. S. & Kurup, V. (1992) *Am. J. Physiol.* **263**, L384–L393.
4. Kato, M. & Staub, N. (1966) *Circ. Res.* **19**, 426–440.
5. Archer, S. L., Huang, J. M. C., Reeve, H. L., Hampl, V., Tolarová, S., Michelakis, E. & Weir, E. K. (1996) *Circ. Res.* **78**, 431–442.
6. Post, J., Hume, J., Archer, S. & Weir, E. (1992) *Am. J. Physiol.* **262**, C882–C890.
7. Yuan, X.-J., Goldman, W., Tod, M. L., Rubin, L. J. & Blaustein, M. P. (1993) *Am. J. Physiol.* **264**, L116–L123.
8. Archer, S. L., Souil, E., Dinh-Xuan, A. T., Schremmer, B., Mercier, J.-C., El Yaagoubi, A., Nguyen-Huu, L., Reeve, H. L. & Hampl, V. (1998) *J. Clin. Invest.* **101**, 2319–2331.
9. Patel, A. J., Lazdunski, M. & Honoré, E. (1997) *EMBO J.* **16**, 6615–6625.
10. Lopez-Barneo, J., Lopez-Lopez, J., Urena, J. & Gonzalez, C. (1988) *Science* **242**, 580–582.
11. Youngson, C., Nurse, C., Yeger, H. & Cutz, E. (1993) *Nature (London)* **365**, 153–155.
12. Zhu, W., Conforti, L., Czyzyk-Krzeska, M. F. & Millhorn, D. E. (1996) *Am. J. Physiol.* **40**, C568–C665.
13. Conforti, L. & Millhorn, D. E. (1997) *J. Physiol.* **502**, 293–305.
14. deMiera, E. V.-S. & Rudy, B. (1992) *Biochem. Biophys. Res. Commun.* **186**, 1681–1687.
15. Reeve, H. L., Weir, E. K., Nelson, D. P., Peterson, D. A. & Archer, S. L. (1995) *Exp. Physiol.* **80**, 825–834.
16. Thomas, H. M. I., Carson, R. C., Fried, E. D. & Novitch, R. S. (1991) *Biochem. Pharmacol.* **42**, R9–R12.
17. Mohazzab-H, K. M. & Wolin, M. S. (1994) *Am. J. Physiol.* **267**, L823–L831.
18. Mohazzab-H, K. M., Fayngersh, R. P., Kaminski, P. M. & Wolin, M. S. (1995) *Am. J. Physiol.* **269**, L637–L644.
19. Cross, A., Henderson, L., Jones, O., Delpiano, M., Hentschel, J. & Acker, H. (1990) *Biochem. J.* **272**, 743–747.
20. Marshall, C., Mamary, A., Verhoeven, A. & Marshall, B. (1996) *Am. J. Resp. Cell. Mol. Biol.* **15**, 633–644.
21. Freeman, B. A. & Crapo, J. D. (1981) *J. Biol. Chem.* **256**, 10986–10992.
22. Archer, S. L., Nelson, D. P. & Weir, E. K. (1989) *J. Appl. Physiol.* **67**, 1903–1911.
23. Paky, A., Michael, J., Burke-Wolin, T. & Wolin, M. (1993) *J. Appl. Physiol.* **74**, 2868–2874.
24. Archer, S., Will, J. & Weir, E. (1986) *Herz* **11**, 127–141.
25. Archer, S. L., Huang, J., Henry, T., Peterson, D. & Weir, E. K. (1993) *Circ. Res.* **73**, 1100–1112.
26. Duchon, M. & Biscoe, T. (1992) *J. Physiol.* **450**, 13–31.
27. Yuan, X.-J., Tod, M., Rubin, L. & Blaustein, M. (1994) *Am. J. Physiol.* **267**, L52–L63.
28. Rounds, S. & McMurtry, I. (1981) *Circ. Res.* **48**, 393–400.
29. Wang, D., Youngson, C., Wong, V., Yeger, H., Dinauer, M., Vega-Salenz de Miera, E., Rudy, B. & Cutz, E. (1996) *Proc. Natl. Acad. Sci. USA* **93**, 13182–13187.
30. Zulueta, J., Sawhney, R., Yu, F., Cote, C. & Hassoun, P. (1997) *Am. J. Physiol.* **272**, L897–L902.
31. Polock, J. D., Williams, D. A., Gifford, M. A. C., Li, L. L., Du, X., Fisherman, J., Orkin, S. H., Doerschuk, C. M. & Dinauer, M. C. (1995) *Nat. Genet.* **9**, 202–209.
32. Jones, S. A., Hancock, J. T., Jones, O. T., Neubauer, A. & Topley, N. (1995) *J. Am. Soc. Nephrol.* **5**, 1483–1491.
33. Umeki, S. (1994) *Life Sci.* **55**, 1–13.
34. Cross, A. & Jones, O. (1986) *Biochem. J.* **237**, 111–116.
35. Stuehr, D., Fasehun, O., Kwon, N., Gross, S., Gonzalez, J., Levi, R. & Nathan, C. (1991) *FASEB J.* **5**, 98–103.
36. Gatley, S. & Sherratt, H. (1976) *Biochem. J.* **158**, 307–315.
37. Weir, E. K., Wyatt, C. N., Reeve, J., Huang, J., Archer, S. L. & Peers, C. (1994) *J. Appl. Physiol.* **76**, 2611–2615.
38. Voelkel, N., Gerber, J., McMurtry, I., Nies, A. & Reeves, J. (1981) *Circ. Res.* **48**, 207–213.
39. Griendling, K. K., Minieri, C. A., Ollerenshaw, J. D. & Alexander, R. W. (1994) *Circ. Res.* **74**, 1141–1148.
40. Archer, S. L., Nelson, D. P. & Weir, E. K. (1989) *J. Appl. Physiol.* **67**, 1912–1921.
41. Rembish, S. J. & Trush, M. A. (1994) *Free Radical Biol. Med.* **17**, 117–126.
42. Archer, S. L., Nelson, D., Gebhard, R., Levine, A., Westcott, J., Voelkel, N., Castleman, R. & Weir, E. K. (1989) *J. Appl. Physiol.* **66**, 1662–1673.
43. Youngson, C., Nurse, C., Yeger, H., Curnutte, J. T., Vollmer, C., Wong, V. & Cutz, E. (1997) *Micro. Res. Tech.* **37**, 101–106.
44. Wenger, R. H., Marti, H. H., Schuerer-Maly, C. C., Kvietikova, I., Bauer, C., Gassman, M. & Maly, F. E. (1996) *Blood* **87**, 756–761.
45. Meier, B., Jesaitis, A., Emmendorffer, A., Roesler, J. & Quinn, M. (1993) *Biochem. J.* **289**, 481–486.
46. Ushio-Fukai, M., Zafari, A. M., Fukui, T., Ishizaka, N. & Griendling, K. K. (1996) *J. Biol. Chem.* **271**, 23317–23321.
47. Jones, S. A., O'Donnell, V. B., Wood, J. D., Broughton, J. P., Hughes, E. J. & Jones, O. T. (1996) *Am. J. Physiol.* **271**, H1626–H1634.
48. Radeke, H. H., Cross, A. R., Hancock, J. T., Jones, O. T., Nakamura, M., Kaefer, V. & Resch, K. (1991) *J. Biol. Chem.* **266**, 21025–21029.
49. Archer, S. L., Hampl, V., Nelson, D. P., Sidney, E., Peterson, D. A. & Weir, E. K. (1995) *Circ. Res.* **77**, 174–181.
50. Mulligan, E., Lahiri, S. & Storey, B. (1981) *J. Appl. Physiol.* **51**, 438–446.
51. Turrens, J., Freeman, B., Levitt, J. & Crapo, J. (1982) *Arch. Biochem. Biophys.* **217**, 401–410.
52. Mills, E. & Jobsis, F. (1972) *J. Neurophysiol.* **35**, 405–428.
53. Obeso, A., Almaraz, L. & Gonzalez, C. (1988) *Brain Res.* **481**, 250–257.
54. Buescher, P., Perse, D., Pillai, R., Litt, M., Mitchell, M. & Sylvester, J. T. (1991) *J. Appl. Physiol.* **70**, 1874–1881.